Passive Seismic Characterization of Salt Jugs near Irsik & Doll Elevators in Hutchinson, Kansas

Shelby Peterie, Julian Ivanov, Richard Miller, Amanda Livers,
Brett Bennett, Bryan Brooks, Joey Fontana,
Brett Judy, Sarah Morton, Jordan Nolan,
Brett Wedel, Yao Wang

Kansas Geological Survey
1930 Constant Avenue
Lawrence, KS 66047

Preliminary Report to

Ed Lindgren and Pete Burton
Burns & McDonnell Engineering Company
9400 Ward Parkway
Kansas City, MO 64114
(816) 822-3138

Open-file Report 2015-29 May 3, 2015

Passive Seismic Characterization of Salt Jugs near the Irsik & Doll Elevators in Hutchinson, Kansas

Executive Summary

This applied research project correlated measured shear-wave velocities with the condition of dissolution voids and the physical properties of the overburden. Shear-wave velocities were estimated using passive surface wave data acquired along four profiles that intersected three wells near the Irsik & Doll grain elevators. Multi-channel analysis of surface waves (MASW) was used to estimate the shear-wave velocity within bedrock, map stratigraphic contacts from and above the top of the "three finger" dolomite, and recommend further investigation where voids are suspected to have the potential for vertical migration and collapse. Qualitative time-lapse analysis is used to interpret changes in shear-wave velocity relative to past investigations at this site and evaluate possible changes in the stress field.

Passive MASW profiles were acquired November 19, 2014, near the Irsik & Doll elevators in Hutchinson, Kansas. Four lines and a surface grid of receivers targeted key wells investigated in previous surveys: 2A, 3B, and 4B. Surface waves with frequencies as low as 4 hertz (Hz) were recorded with an average depth of investigation of 60 meters (m), successfully sampling to a significant depth within bedrock.

With shear-wave velocity being a function of shear modulus and density (the shear modulus is the ratio of stress over strain), it is possible to quantify relative stress of overburden rocks (shear modulus) by shear velocity values. Local increases in shear velocity without changes in lithology can be equated to increased stress associated with overburden roof load over dissolution jugs. Relative shear velocity lows may be associated with collapse features whose vertical movement has been arrested by bulking, reduced stress to within roof rock strength, or changes in strength due to geologic features related to natural variation in deposition or erosion. Comparative analysis of relative changes in shear velocity between successive surveys may provide qualitative insight in temporal variability of stress associated with voids.

Shear velocities and surface wave dispersion patterns over wells 3B and 4B are mostly consistent with past surveys and likely indicative of a normal stress regime and natural geologic variation. However, a possible temporal decrease in bedrock velocity at a depth of 70 m may warrant further investigation to increase confident in the interpretation at well 3B. A horizontal and temporal decrease in shear velocity at well 2A suggests possible roof rock failure and reduced strength in the overlying bedrock. Although this anomalous shear velocity zone could be attributed to lithology that was poorly resolved in the previous surveys (e.g. depositional variation), a temporal change in the dispersion patterns at well 2A supports vertical migration of the void. Additional geotechnical and/or seismic investigations are required to improve confidence in the interpretation.

Introduction

Material properties (specifically strength and stress accumulations) measured as a function of depth above abandoned salt jugs in Hutchinson, Kansas, appear to be related to the mobility and upward migration potential of these jugs. Localized increases in stress (as indicated by increased shear-wave velocity) above subterranean voids is one indicator of an increased potential for roof failure and void migration (Eberhart-Phillips et al., 1989; Dvorkin et al., 1996; Khaksar et al., 1999; Sayers, 2004). Previous studies, using both active and passive seismic wavefield characteristics, suggest that perturbations in the shear-wave velocity field immediately above voids can be correlated to characteristics of the unsupported roof spans of salt jugs in this area (Sloan et al., 2010).

The strength of individual rock layers can be qualitatively described in terms of stiffness/ rigidity and empirically estimated from relative comparisons of shear-wave velocity measurements. Shear-wave velocity is directly proportional to stress and inversely related to non-elastic strain. Since the shear-wave velocity of earth materials changes when stress and any associated elastic strain on those materials becomes "large," it is reasonable to suggest load-bearing roof rock above mines or dissolution voids may experience elevated shear-wave velocities due to loading between pillars or, in the case of voids, loading between supporting side walls. This localized increase in shear velocity is not related to increased strength, but increased load as defined by Young's Modulus. High-velocity shear-wave "halos" encompassing low-velocity anomalies are suggested to be key indicators of near-term roof failure. All these phenomena have been observed at this Hutchinson site at depths greater than 30 m below the bedrock surface.

Previous active seismic reflection experiments at this site have detected areas with elevated shear-wave velocity likely indicative of an imminent risk for vertical migration of specific salt jugs (Sloan et al., 2010). The lack of necessary ultra low-frequency surface waves in the recorded wavefield have negated attempts to use active source MASW to estimate shear velocity in the lithified rocks near the top of bedrock (Miller et al., 2009). Uncontrolled, local industrial and transportation activities represent sound sources that have produced the necessary low frequencies and, when recorded and processed using passive methods, have extended the imaging depth to over 200 feet (ft) (Miller, 2011).

Passive surface-wave recording allows random sources of seismic energy (trains, manufacturing facilities, heavy vehicles on roadways, processing plants, heavy construction equipment, etc.), considered noise on active surveys, to be recorded so that data processing enhancements and specialized processing methods can be used to calculate the 1-D shear wave velocity function. The key to this method is the ability to estimate shear-wave velocities to depths double or more than otherwise possible with standard active sources at a particular site (Park et al., 2004). Results of past studies at this site suggest the method is effective in predicting jugs with heightened risk for upward migration (Miller, 2011; Ivanov et al., 2013)

Three previous 2-D passive MASW surveys were acquired near the Irsik & Doll elevators in 2012 and 2013. Results of these investigations largely suggested a normal stress regime with natural geologic variation. Time-lapse analysis can be used to monitor for temporal variation in shear velocity. A temporal reduction observed in the shear velocity associated with a given well may be used to identify voids that have vertically migrated during the time that elapsed between successive surveys.

Geologic and Geophysical Setting

The Permian Hutchinson Salt Member occurs in central Kansas, northwestern Oklahoma, and the northeastern portion of the Texas Panhandle, and is prone to and has an extensive history of dissolution and formation of sinkholes (Figure 1). In Kansas, the Hutchinson Salt Member possesses an average net thickness of 75 m and reaches a maximum of over 150 m in the southern part of the basin. Deposition occurring during fluctuating sea levels caused numerous halite beds, 0.2 to 3 m thick, to be formed interbedded with shale, minor anhydrite, and dolomite/magnesite. Individual salt beds may be continuous for only a few miles despite the remarkable lateral continuity of the salt as a whole (Walters, 1978).

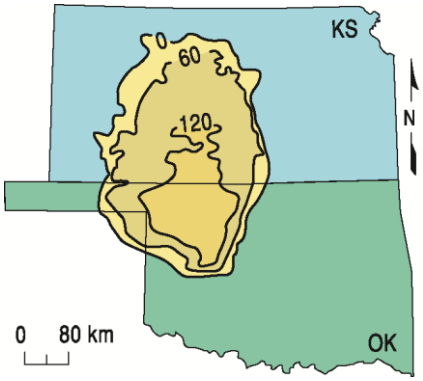

Figure 1. Approximate extent of salt formation, with contour intervals expressed in meters.

The distribution and stratigraphy of the salt is well documented (Dellwig, 1963; Holdo-way, 1978; Kulstad, 1959; Merriam, 1963). The salt reaches a maximum thickness in central Oklahoma and thins to depositional edges on the north and west, erosional subcrop on the east, and facies changes on the south. The increasing thickness toward the center of the salt bed is due to a combination of increased salt, and more and thicker interbedded anhydrites. The Stone Corral Formation (a well documented seismic marker bed) overlies the salt throughout Kansas (McGuire and Miller, 1989). Directly above the salt at this site is a thick sequence of Permian shales.

The upper 760 m of rock at this site is Permian shale (Merriam, 1963). The Chase Group (top at 300 m deep), lower Wellington Shale (top at 245 m deep), Hutchinson Salt (top at 120 m deep), upper Wellington Shale (top at 75 m deep), and Ninnescah Shale (top at 25 m deep) make up the packets of reflecting events easily identifiable and segregated within the Permian portion of the section (Figure 2). Bedrock is defined as the top of the Ninnescah Shale with the unconsolidated Pliocene-Pleistocene Equus beds making up the majority of the upper 30 m of sediment. The thickness of Quaternary alluvium that fills the stream valleys and paleosubsidence features goes from 0 to as much as 90 m, depending on the dimensions of the features.

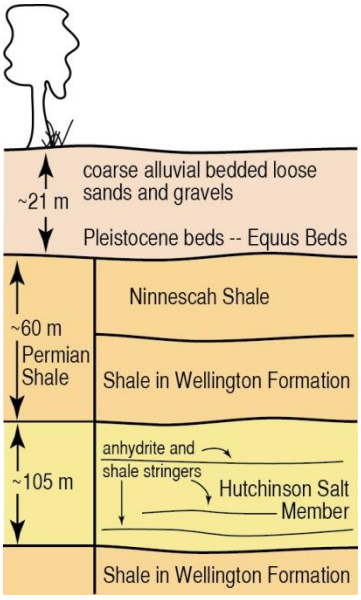

Figure 2. Generalized geology.

Recent dissolution of the salt and resulting subsidence of overlying sediments forming sinkholes has generally been associated with mining or saltwater disposal (Walters, 1978). Historically, these sinkholes can manifest themselves as a risk to surface infrastructure. The rate of surface subsidence can range from gradual to very rapid. Besides risks to surface structures, subsidence features potentially jeopardize the natural segregation of ground-water aquifers, greatly increasing their potential to negatively impact the environment (Whittemore, 1989, 1990). Natural sinkholes resulting from dissolution of the salt by localized leaching within natural flow systems which have been

altered by structural features (such as faults and fractures) are not uncommon west of the main dissolution edge (Merriam and Mann, 1957).

Caprock and its characteristics are a very important component of any discussion concerning dissolution, subsidence, and formation of sinkholes. The Permian shales (Wellington and Ninnescah) that overlay the Hutchinson Salt Member are about 60 m thick in this area and are characterized as generally unstable when exposed to freshwater, being susceptible to sloughing and collapse (Swineford, 1955). These Permian shales tend to be red or reddish-brown and are commonly referred to as "red beds." Permian red beds are extremely impermeable to water and have therefore provided an excellent seal between the freshwaters of the Equus beds and the extremely water-soluble Hutchinson Salt Member. The modern-day expanse and mere presence of the Hutchinson Salt is due to the protection from freshwater provided by these red beds.

Isolating the basal contact of the Wellington Formation provides key insights into the general strength of roof rock expected if dissolution-mined salt jugs (salt jugs are the cavities or voids, many times shaped like jugs, in the salt that form after salt has been dissolution mined in proximity to the wells) reach the top of the salt zone. Directly above the salt/shale contact is an approximately 6-m-thick dark-colored shale with joint and bedding cracks filled with red halite (Walters, 1978). Once unsaturated brine comes in contact with this shale layer, these red halite-filled joints and bedding planes are rapidly leached, leaving an extremely structurally weak layer.

Study IV: Follow-up investigation of wells 2A, 3B, and 4B

Field Layout and Data Acquisition

A fourth survey was performed on November 19, 2014 to monitor for relative changes in shear-wave velocity and enhance the interpretation at wells 2A, 3B, and 4B. Four 1-D lines and a 2-D grid of receivers were deployed in the study area (Figure 3). As in the previous surveys, seismic receivers were single GeoSpace GS11D 4.5 Hz vertical geophones. The 1-D seismic lines varied in length (Table 1), totaling almost 1 kilometer (km) with receivers spaced at 3 m intervals. Data were recorded continuously during one night with a 400+ channel 24-bit Geometrics Geode distributed seismic system. Seismic records were 32 seconds (s) long with a 2 millisecond (ms) sampling interval. In total, 783 seismic records equivalent to 21.3 gigabytes (Gb) of data were recorded.

Table 1. Number of receivers and total line lengths for the 1-D seismic lines.

	line 2	line 10	line 11	line 56
number of receivers	96	72	96	72
total length (m)	285	213	285	213

Processing and Analysis

Data were processed using algorithms developed at the KGS. The general processing flows are consistent with those used for previous surveys. The passive method used for this study is well established and provided good quality results at this site (Park et al., 2004; Ivanov et al., 2013). Caution is required when comparing velocity profiles from different surveys. Variations in data quality (i.e. signal-to-noise ratio), source characteristics (e.g. orientation, weight, speed), and other differences between time-lapse surveys (e.g. seasonal variations) can contribute to

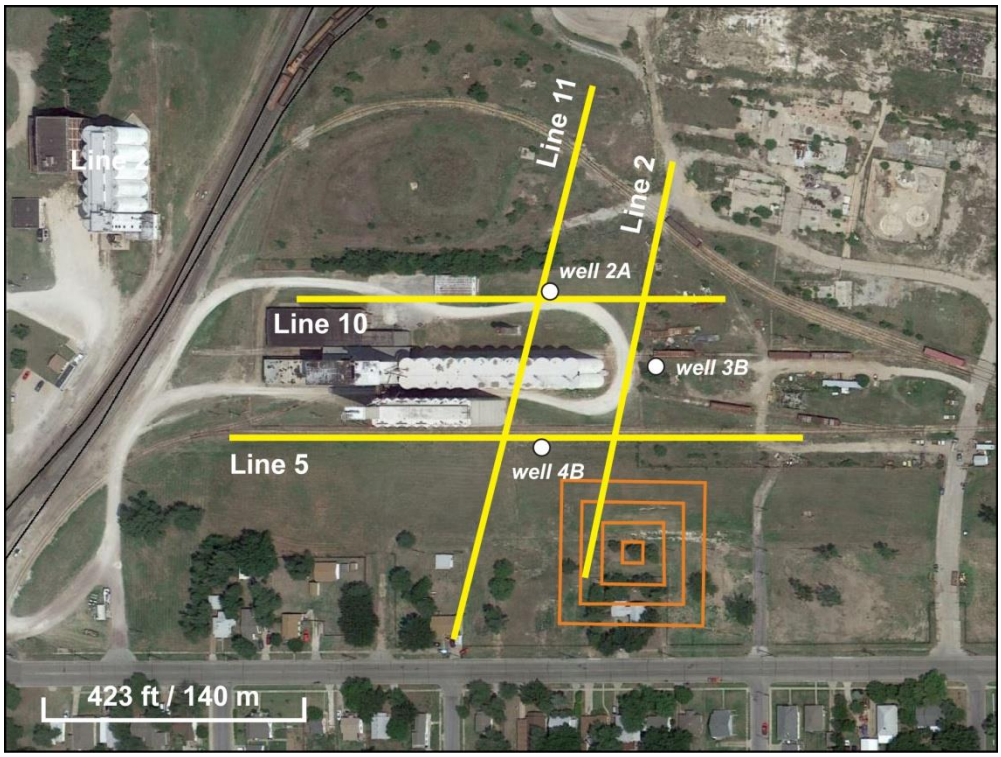

Figure 3. Aerial photo indicating GPS locations of seismic lines (yellow), 2-D monitoring grid (orange) and locations of wells in the study area (white) from the November 2014 survey.

uncertainty and overall differences and in resulting 2-D shear velocity profiles. In general, time-lapse analyses are intended to be relative comparisons.

Continuous acquisition records energy from energy sources at various orientations with respect to the seismic line. The 2-D grid was deployed to evaluate and optimize source alignment with respect to each 1-D seismic line. For each line, the surface wave amplitudes recorded by the 2-D grid were plotted as phase velocity versus frequency for a range of azimuths from 0 to 360 degrees with respect to the seismic line to determine which record had the best broad band, low frequency source with an azimuth near parallel to the line (Figure 4). The seismogram with optimum source characteristics was selected and divided into the shortest groups of receivers ("spread length") determined to provide dispersion patterns on phase velocity versus frequency plots with high amplitude fundamental mode Rayleigh wave energy and minimal higher-order surface wave interference (Figure 5). Fundamental mode dispersion curves were picked and inverted to obtain a 2-D section of shear wave velocity (V_s) as a function of depth. The apparent velocity (v_{app}) is:

$$v_{app} = \frac{v_{act}}{(\cos\theta)} \tag{1}$$

where v_{act} is the actual seismic velocity and θ is the azimuth of the source with respect to the seismic line determined from the azimuth versus frequency plot. Thus, the increase in velocity (Δv) is:

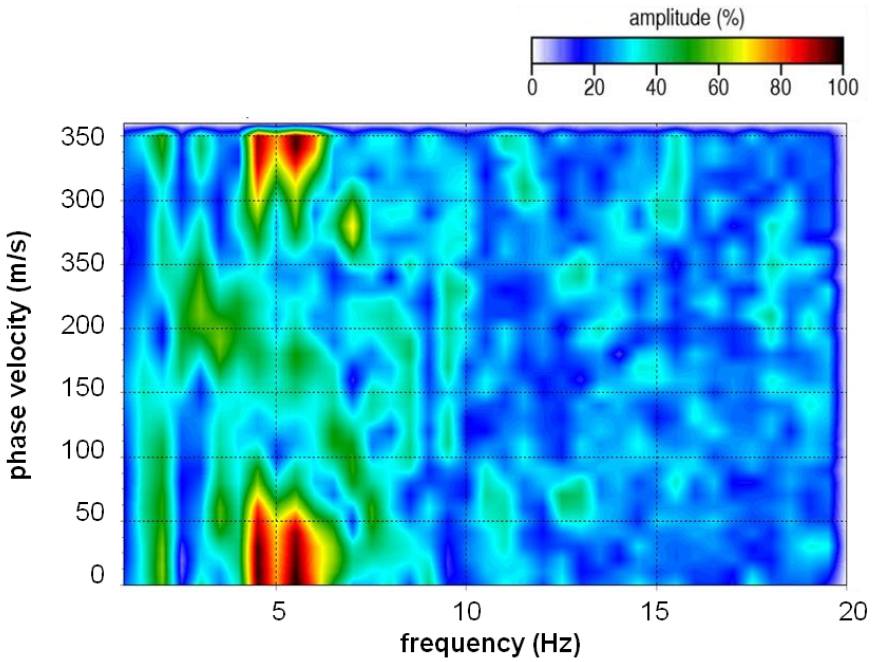

Figure 4. Azimuth plot indicating the direction of the dominant passive source energy (in degrees counter-clockwise from east). Here, the dominant passive source energy is centered on 350°.

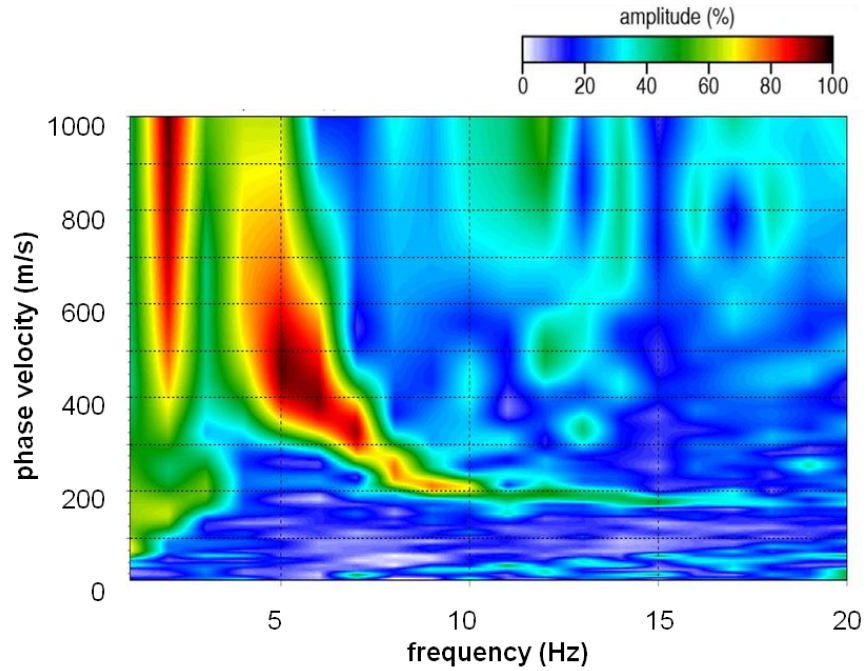

Figure 5. Representative dispersion pattern with high signal-to-noise ratio of the fundamental mode Rayleigh wave.

$$\Delta v = \frac{1}{\cos\theta} - 1 \quad (2)$$

Equation 2 was used to calculate the increase in velocity due to the source azimuth for each line (Table 2).

Table 2. Orientation of the passive seismic sources and the seismic lines (in degrees counterclockwise from east), the angle of the source with respect to the line (θ), and the percent increase in apparent velocity caused by oblique source orientations (Δv).

line	source orientation	line orientation	θ	Δv
2	270°	255°	15°	4 %
5	10°	1°	9°	1 %
10	350°	0°	10°	2 %
11	275°	254°	21°	7 %

Results

The 2-D velocity profiles from the current study and past surveys are presented below and discussed in detail in the following section. To achieve more comparable velocities on line 5, the original October 2012 dispersion curves were reprocessed with the same algorithm and general parameters used for this study. Dispersion curves were not re-picked, but simply re-inverted with improved parameters consistent with the November 2014 survey. Line 2, 10, and 11 profiles are the original results from past surveys.

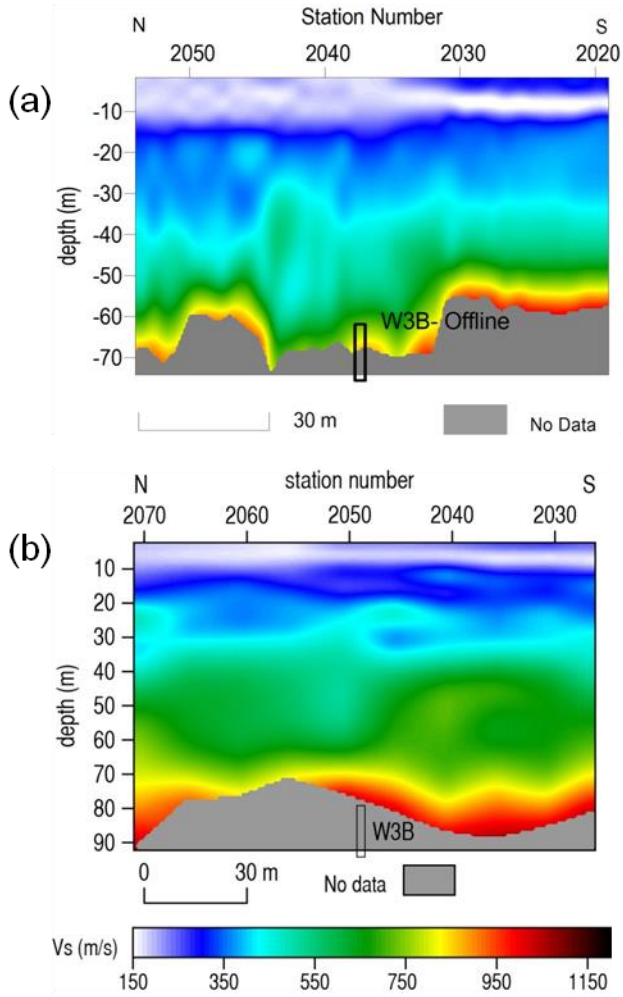

Figure 6. Final line 2 shear-wave velocity profile from (a) November 2014 and (b) August 2012. Approximate well location is indicated at the bottom of the profiles.

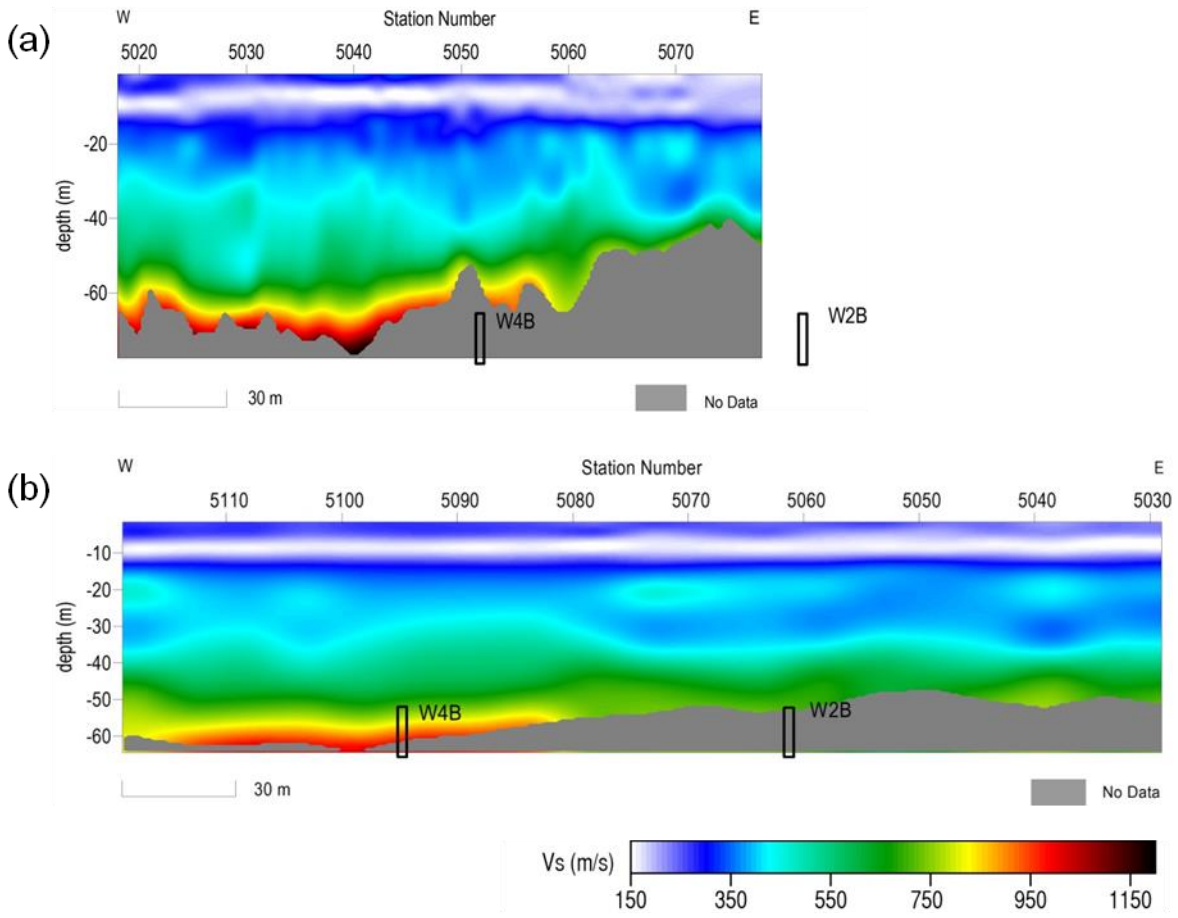

Figure 7. Final line 5 shear-wave velocity profile from (a) November 2014 and (b) October 2012. Approximate well locations are indicated at the bottom of the profiles.

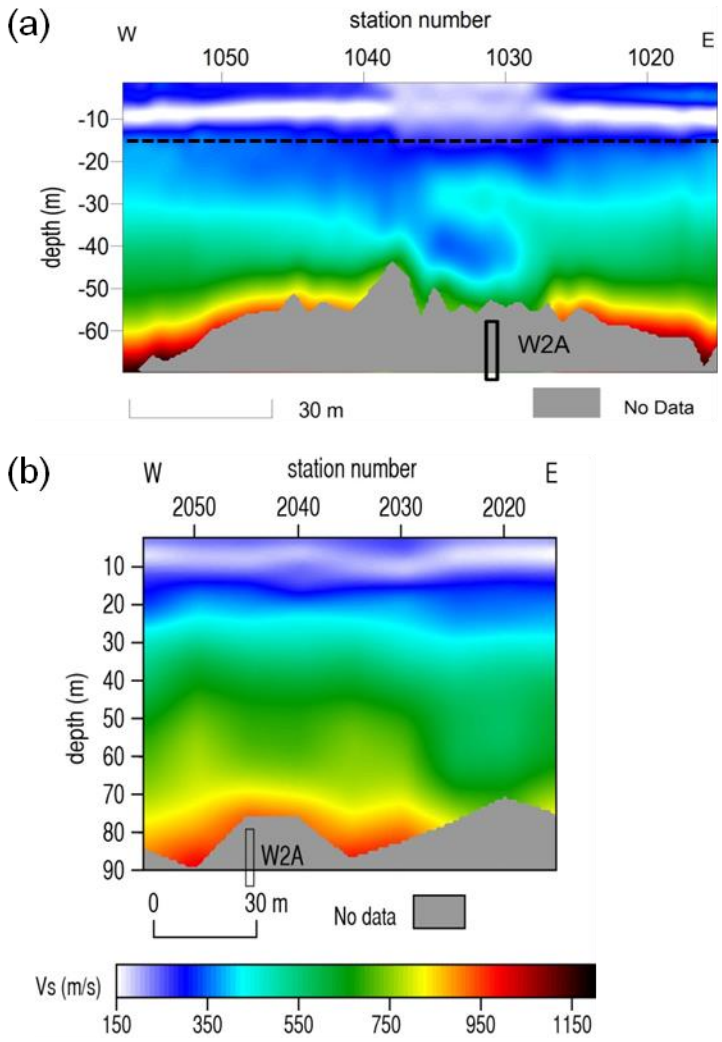

Figure 8. Final line 10 shear-wave velocity profile from (a) November 2014 and (b) March 2013. Approximate well location is indicated at the bottom of the profiles. The black line represents the shallowest depth sampled.

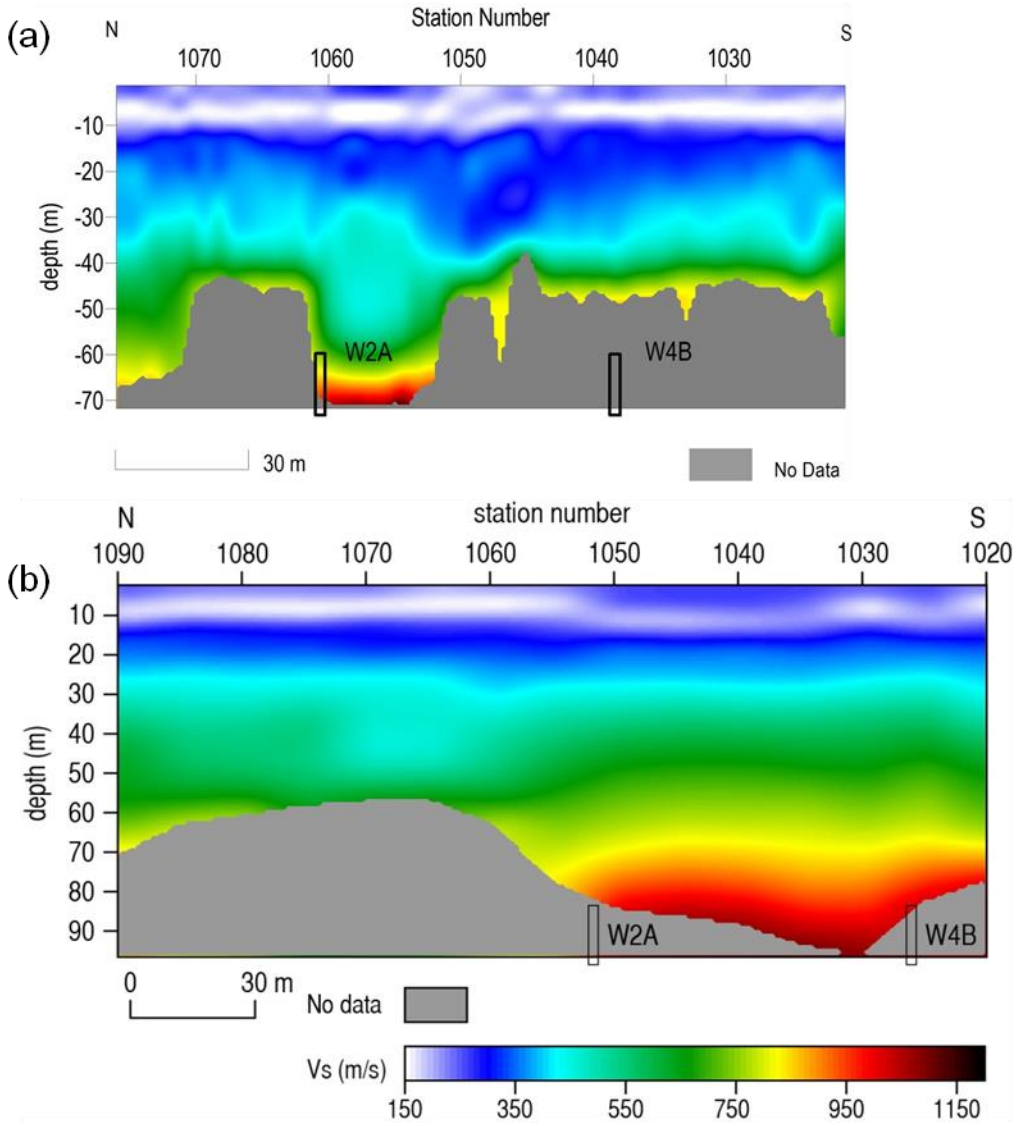

Figure 9. Final line 11 shear-wave velocity profile from (a) November 2014 and (b) March 2013. Approximate well locations are indicated at the bottom of the profiles.

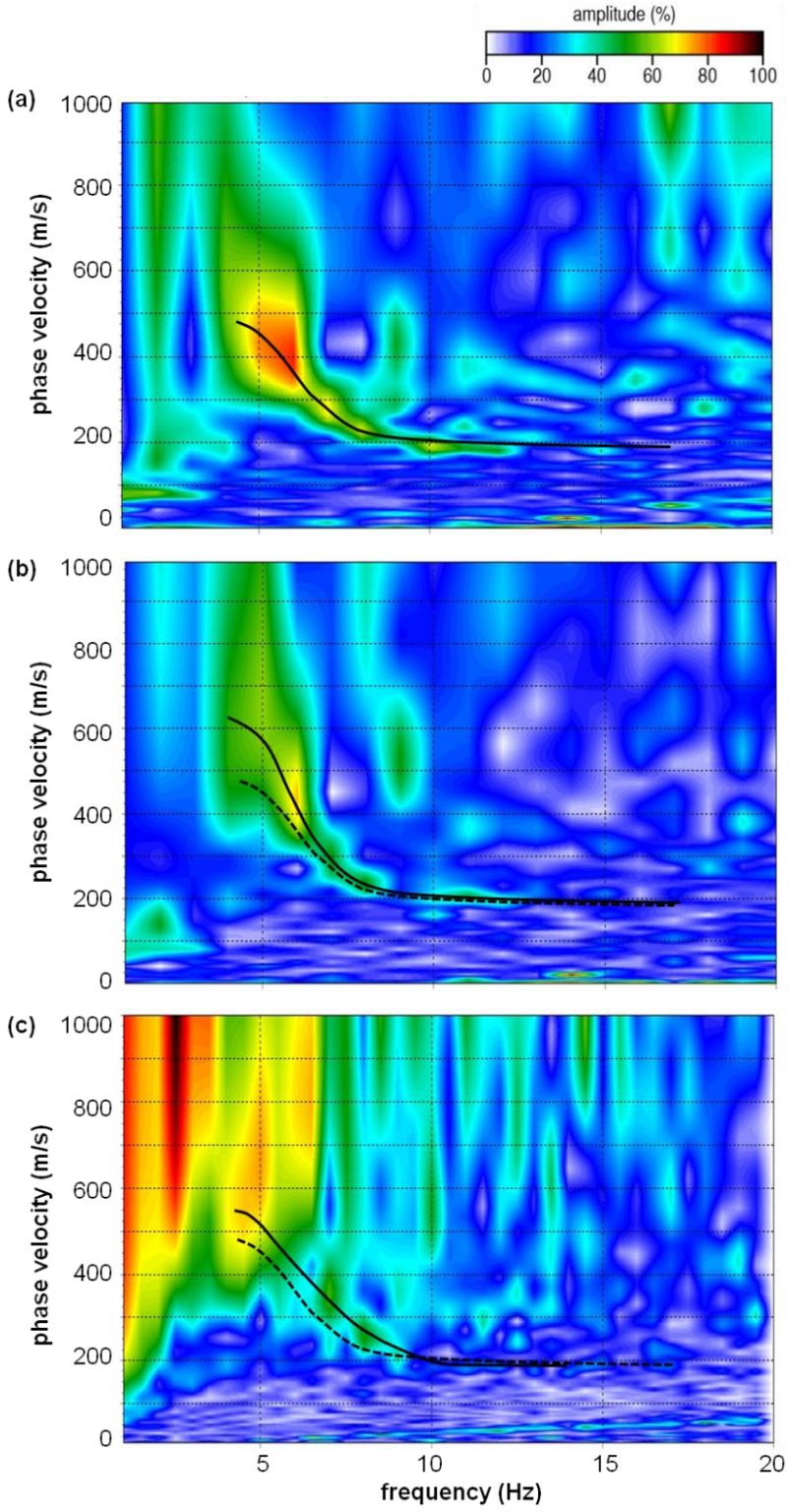

Figure 10. Dispersion pattern from line 10 (a) at well 2A, November 2014; (b) from the west end of the line, November 2014; and (c) at well 2A, March 2013. Approximate picked dispersion curves (solid black line) are superimposed on the dispersion images. The dispersion curve in (a) is superimposed on (b) and (c) (dashed black line).

Interpretation and Discussion

Line 2 is oriented N-S and is located 20 m east of the elevator and 5 m west of well 3B. During the August 2012 survey, the seismic source was oriented approximately 30° with respect to the seismic line, resulting in a ~15% uniform increase in velocity. The decrease in velocity observed on the November 2014 2-D profile (Figure 6a) relative to the August 2012 profile (Figure 6b) is most likely attributable to the difference in source orientation. Lateral variability in bedrock velocity is consistent on both lines; although, it is better defined on the profile from the current study due to increase horizontal sampling used in processing. A horizontal decrease in bedrock velocity is located near well 3B. Dispersion curves suggest that bedrock velocity at a depth of 70 m at this location may be lower than in August 2012, even when the difference in source orientation is accounted for. Although line 2 is mostly consistent with the previous study and likely represents natural geologic variation (as previously interpreted), the coincidental location of well 3B and a horizontal and possible temporal decrease in bedrock velocity may warrant further investigation to improve confidence in the interpretation.

Line 5 was deployed with a W-E orientation approximately 25 m south of the elevator. A gentle velocity gradient is observed increasing to the west (Figure 7a). The absolute velocities and the general velocity trend observed in the present study are very similar to the re-inverted October 2012 profile (Figure 7b). The geometry and relative velocity of this gentle gradient and lack of temporal change is suggestive of a natural variation in geology and a normal stress regime.

Line 10 was deployed with a W-E orientation over well 2A approximately 30 m north of the grain elevators. Line 11 was deployed with a N-S orientation over well 2A and approximately 15 m west of well 4B. On line 11 (Figure 9b), the bedrock velocity at well 4B is consistent with bedrock velocity on other lines at this site, likely indicating a normal stress regime associated with this well.

A 20-30% decrease in the shear velocity of bedrock centered on well 2A is observed on both lines 10 (Figure 8a) and 11 (Figure 9a) that was not observed during the previous studies (Figures 8b and 9b, respectively). The surface wave dispersion pattern on line 10 at well 2A (Figure 10a) indicates lower surface wave phase velocities relative to the west end of the line (Figure 10b) at frequencies lower than 7 Hz. Using the half-wavelength approximation:

$$z \approx \frac{\lambda}{2} = \frac{v}{2f} \tag{3}$$

the depth of investigation of surface waves with a frequency of 7 Hz and a velocity of 275 meters per second (m/s) is approximately 20 m. This indicates that the decrease in shear velocity is confined to roughly 20 m and deeper, beneath the top of bedrock. Although it appears there is a horizontal change in material properties above bedrock at this location, short wavelength surface waves corresponding to these shallow depths were not recorded (due to the low-frequency nature of the passive seismic source). Therefore, velocities above 10-15 m are uncertain and the horizontal change in velocity above this depth is an inversion artifact.

Without additional information from other geotechnical methods, the anomalous shear velocity in the bedrock near well 2A could have several interpretations. The high velocity at 25 m underlain by lower velocity at 40 m could represent depositional variation. If this were the case, it would likely have been observed in the March 2013 velocity profile (Figures 8b and 9b). Although the fundamental mode Rayleigh wave has a lower signal-to-noise ratio in the March

2013 dataset, it appears the dispersion pattern directly over well 2A had a higher velocity trend than in the present study (Figure 10c). This suggests a change in material properties between the two surveys.

Lack of surface wave sampling below 55 m near well 2A on line 10 could suggest failure of roof rock, decreased velocity and, because wavelength is proportional to velocity (equation 3), reduced depth of investigation. However, surface waves sample down to 70 m at this location on line 11. On this line, this represents an increase in the surface wave propagation depth relative to the rest of the line. This may indicate increased velocity and elevated stress at this location.

Observations from lines 10 and 11 in the present and past studies are consistent with upward migration of the void roof. Although there are other possible interpretations (e.g. variation in lithology that was poorly resolved in past surveys), temporal changes in the dispersion patterns at well 2A support the possibility of roof rock failure and loss of strength in the overlying bedrock. If some degree of roof rock failure did occur, lack of elevated velocity/stress at the top of bedrock may indicate that vertical migration is currently halted and the void has stabilized. Additional geotechnical and/or seismic investigations are required to improve confidence in the interpretation.

Conclusions

The bedrock velocity trends on lines 2 and 5 are generally consistent with the shear velocity expected at this site and likely represent a normal stress regime at wells 3B and 4B, respectively. A possible temporal decrease in bedrock velocity at a depth of 70 m on line 2 may warrant further investigation to increase confident in the interpretation at well 3B.

A horizontal and temporal decrease in shear velocity at well 2A suggests possible roof rock failure and reduced strength in the overlying bedrock. Although this anomalous shear velocity zone could be attributed to lithology that was poorly resolved in the previous surveys (e.g. depositional variation), a temporal change in the dispersion patterns at well 2A on line 10 supports vertical migration of the void roof upwards. We are defining roof here as the lowest portion of the rock over the void that has retained background strength. There might still be residual material along the top of the void that has not collapsed but provides no strength to support the overburden. That is not to suggest that the roof has physically collapsed, but that there seems to have been some kind of failure that has reduced the strength of the overburden below 150 ft.

It is also possible void migration halted when the void space filled with collapse breccia and that occurred prior to surface expression. Since we don't see an increase in stress at the top of bedrock it does not seem likely that a surface depression is imminent. A loss of strength (drop in shear velocity) could have occurred and the void has currently stabilized until the stress builds sufficiently to continue the migration.

Additional geotechnical and/or seismic investigations are required to improve confidence in the interpretation.

References

Dellwig, L.F., 1963, Environment and mechanics of deposition of the Permian Hutchinson Salt Member of the Wellington shale: Symposium on Salt, Northern Ohio Geological Society, p. 74-85.

Dvorkin, J., A. Nur, and C. Chaika, 1996, Stress sensitivity of sandstones: *Geophysics*, v. 61, p. 444-455.

Eberhart-Phillips, D., D.-H. Han, and M.D. Zoback, 1989, Empirical relationships among seismic velocity, effective pressure, porosity, and clay content in sandstone: *Geophysics*, v. 54, p. 82-89.

Holdoway, K.A., 1978, Deposition of evaporites and red beds of the Nippewalla Group, Permian, western Kansas: Kansas Geological Survey Bulletin 215.

Ivanov, J., R.D. Miller, S.L. Peterie, J.T. Schwenk, J.J. Nolan, B. Bennett, B. Wedel, J. Anderson, J. Chandler, and S. Green, 2013, Enhanced Passive Seismic Characterization of High Priority Salt Jugs in Hutchinson, Kansas: preliminary report to Burns & McDonnell Engineering Company.

Khaksar, A., C.M. Griffiths, and C. McCann, 1999, Compressional- and shear-wave velocities as a function of confining stress in dry sandstones: *Geophysical Prospecting*, v. 47, p. 487-508.

Kulstad, R.O., 1959, Thickness and salt percentage of the Hutchinson salt; in, Symposium on Geophysics in Kansas: Kansas Geological Survey Bulletin 137, p. 241-247.

McGuire, D., and B. Miller, 1989, The utility of single-point seismic data: In Geophysics in Kansas, D.W. Steeples, ed.: Kansas Geological Survey Bulletin 226, p. 1-8.

Merriam, D.F., 1963, The Geologic History of Kansas: Kansas Geological Survey Bulletin 162, 317 p.

Merriam, D.F., and C.J. Mann, 1957, Sinkholes and related geologic features in Kansas: Transactions of the Kansas Academy of Science, v. 60, p. 207-243.

Miller, R.D., 2011, Progress report: 3-D passive surface-wave investigation of solution mining voids in Hutchinson, Kansas: Interim report to Burns & McDonnell Engineering Company, January, 9 p.

Miller, R.D., J. Ivanov, S.D. Sloan, S.L. Walters, B. Leitner, A. Rech, B.A. Wedel, A.R. Wedel, J.M. Anderson, O.M. Metheny, and J.C. Schwarzer, 2009, Shear-wave study above Vig-industries, Inc. legacy salt jugs in Hutchinson, Kansas: Kansas Geological Survey Open-file Report 2009-3.

Park, C., R. Miller, D. Laflen, N. Cabrillo, J. Ivanov, B. Bennett, and R. Huggins, 2004, Imaging dispersion curves of passive surface waves [Exp. Abs.]: Annual Meeting of the Soc. of Expl. Geophys., Denver, Colorado, October 10-15, p. 1357-1360.

Sayers, C.M., 2004, Monitoring production-induced stress changes using seismic waves [Exp. Abs.]: Annual Meeting of the Soc. of Expl. Geophys., Denver, Colorado, October 10-15, p. 2287-2290.

Sloan, S.D., S.L. Peterie, J. Ivanov, R.D. Miller, and J.R. McKenna, 2010, Void detection using near-surface seismic methods; *in* Advances in Near-Surface Seismology and Ground-Penetrating Radar, SEG Geophysical Developments Series No. 15, R.D. Miller, J.D. Bradford, and K. Holliger, eds.: Tulsa, Society of Exploration Geophysicists, p. 201-218.

Swineford, A., 1955, Petrography of upper Permian rocks in south-central Kansas: State Geological Survey of Kansas Bulletin 111, 179 p.

Walters, R.F., 1978, Land subsidence in central Kansas related to salt dissolution: Kansas Geological Survey Bulletin 214, 82 p.

Whittemore, D.O., 1990, Geochemical identification of saltwater contamination at the Siefkes subsidence site: Report for the Kansas Corporation Commission.

Whittemore, D.O., 1989, Geochemical characterization of saltwater contamination in the Macksville sink and adjacent aquifer: Kansas Geological Survey Open-file Report 89-35.